Chinese Chemical Letters 35 (2024) 109261

Contents lists available at ScienceDirect

Chinese Chemical Letters

journal homepage: www.elsevier.com/locate/cclet

Modification strategies for non-aqueous, highly proton-conductive benzimidazole-based high-temperature proton exchange membranes

Yunfa Dong[a], Shijie Zhong[a], Yuhui He[a], Zhezhi Liu[b], Shengyu Zhou[a], Qun Li[a], Yashuai Pang[c], Haodong Xie[a], Yuanpeng Ji[d,e], Yuanpeng Liu[a], Jiecai Han[a], Weidong He[a,e,f,*]

[a] National Key Laboratory of Science and Technology on Advanced Composites in Special Environments, and Center for Composite Materials and Structures, Harbin Institute of Technology, Harbin 150080, China
[b] School of Petroleum Engineering, Chongqing University of Science and Technology, Chongqing 401331, China
[c] School of Physics, University of Electronic Science and Technology of China, Chengdu 610054, China
[d] MIIT Key Laboratory of Critical Materials Technology for New Energy Conversion and Storage, School of Chemistry and Chemical Engineering, Harbin Institute of Technology, Harbin 150001, China
[e] Chongqing Research Institute, Harbin Institute of Technology, Chongqing 401151, China
[f] School of Mechanical Engineering, Chengdu University, Chengdu 610106, China

ARTICLE INFO

Article history:
Received 6 July 2023
Revised 25 October 2023
Accepted 26 October 2023
Available online 30 October 2023

Keywords:
Benzimidazole
Nonaqueous proton conduction
Free volume
Nanophase-separated structure
Structure modification

ABSTRACT

High-temperature proton exchange membranes (HT-PEMs) possess excellent thermal and outstanding electrochemical stability, providing an avenue to realize high-temperature proton exchange membranes fuel cells (HT-PEMFCs) with both superior power density and long-term durability. Unfortunately, polybenzimidazole (PBI), a typical material for conventional HT-PEMs, fails to compromise the high nonaqueous proton conductivity and high mechanical properties, thus hindering their practical applications. Achieving efficient nonaqueous proton conduction is crucial for HT-PEMFC, and many insightful research works have been done in this area. However, there still lacks a report that integrates the host-guest interactions of phosphoric acid doping and the structural stability of polymers to systematically illustrate modification strategies. Here, we summarize recent advancements in enhancing the nonaqueous proton conduction of HT-PEMs. Various polymer structure modification strategies, including main chain and side group modification, cross-linking, blocking, and branching, are reviewed. Composite approaches of polymer, including compounding with organic porous polymers, filling the inorganic components and modifying with ionic liquids, *etc*., are also covered in this work. These strategies endow the HT-PEMs with more free volume, nanophase-separated structure, and multi-stage proton transfer channels, which can facilitate the proton transportation and improve their performance. Finally, current challenges and future directions for further enhancements are also outlined.

1. Introduction

Proton exchange membrane fuel cell (PEMFC) is one of the most ideal alternatives to the internal combustion engine due to its high efficiency, low emission, compact cell design, and no pollution to the environment [1–4]. One of the most important parts of PEMFC is the proton exchange membrane, which acts as the solid electrolyte of the battery to prevent the cross-mixing of fuel and oxidizer and to allow proton transfer between the cathode and anode [5–8]. At low temperatures (<100 °C), the current commercialized proton exchange membrane is Nafion for its superior mechanical properties, high proton transfer efficiency, and excellent chemical inertness below 80 °C. However, it also has fatal disadvantages, such as high dependence on water in proton conduction, resulting in difficulties in heat and water management, high methanol penetration, and high cost, which limit its large-scale application [9–14]. Compared to traditional PEMFC at low temperatures (<100 °C), the HT-PEMFC which is running under the condition of high temperatures (100–200 °C) and low humidity has aroused people's great interest because of the impressive features, such as reduced possibility of carbon monoxide poisoning of the anode catalyst, greater catalytic activity, streamlined management of H_2O/heat and enhanced compatibility to H_2 contaminants [15–19]. Moreover, HT-PEMFCs can use high energy density liquid fuels such as methanol to produce hydrogen, which can reduce the weight of the fuel cell system by 37.5%, endowing the HT-PEMFCs with extensive ap-

* Corresponding author.
E-mail address: weidong.he@hit.edu.cn (W. He).

https://doi.org/10.1016/j.cclet.2023.109261
1001-8417/

plication prospects. However, there are no mature, commercially available HT-PEMs [20,21]. Therefore, the development of an inexpensive material that can be utilized at HT-PEMFC is imminent, which requires game-changing technology from PEM research for HT-PEMFCs.

There are many candidates for HT-PEM materials, such as metal-organic frameworks (MOFs), covalent organic frameworks (COFs), polymers and inorganic materials, among which polybenzimidazole (PBI) is the most promising. Thanks to the rich proton conduction sites of nitrogen-containing heterocycles and the rigid backbone, PBI has the following advantages: exceptional mechanical strength, excellent thermodynamic and chemical stability [22,23]. PBI has a unique alkaline heterocyclic structure, which can uptake a substantial quantities of phosphoric acid (PA), and still maintain superior mechanical properties and powerful ability to isolate hydrogen gas after adsorption of phosphoric acid [24]. There are two main methods for preparing phosphoric acid doped PBI membranes, one is to polymerize the monomer in polyphosphoric acid and directly prepare phosphoric acid doped PBI membranes using the phosphoric acid generated by hydrolysis [25]. The other is to prepare the PBI membrane first, and then phosphoric acid absorption is followed [26]. Although the process of the polyphosphoric acid method is relatively simple, the purity requirement for monomer is high, the large amount of phosphoric acid generated by hydrolysis poses a challenge to the regulation of the film formation process, and the mechanical properties of the PBI film obtained by this method are poor. Since a variety of PBIs with good solubility in organic solvents have been prepared, the method of film formation followed by phosphoric acid adsorption is more suitable. The proton transportation ability of membrane acts as a crucial factor in determining the final performance of the fuel cell. Therefore, how to improve the proton transmission efficiency of the membrane has always been a core topic in the field of novel PBI-based membranes. For the PA-PBI architecture under high temperature and water-free operating circumstances, the proton conduction mainly follows the Grotthuss mechanism, and the proton mainly jumps and conducts in the hydrogen bond network of PA [27]. The nonaqueous proton conduction of the PA-doped PBI architecture is primarily affected by the PA doping level (ADL). However, most of the reported PBI-based PEMs, due to the plasticization of PA molecules will lead to poor mechanical properties, especially at high ADL, thus, it cannot meet the requirements of practical applications [28]. Therefore, how to realize efficient proton conduction while maintaining the mechanical strength of PBI remains a challenge.

So far, reviews on high-temperature proton exchange membranes have focused on summarizing structural modifications of polymers [18,22,29,30], inorganic particle doping [9,31–33], and ionic liquid modifications [5,34–36], respectively, and to our knowledge, there is no report that integrates the host-guest interactions of phosphoric acid doping and the structural stability of polymers to systematically illustrate modification strategies. Improving the anhydrous proton conductivity of HT-PEMs requires a case-by-case breakthrough from the influencing factors that affect membrane proton conductivity. Generally speaking, there are three main influencing factors. The number of PA doping sites decided the efficiency of proton conduction, while the long-term retention rate after phosphoric acid doping affects the stability of proton conduction [37]. It is worth noting that the balance and restriction relationship between proton conductivity and mechanical properties usually make a big difference [38].

As shown in Fig. 1a [39–44], this paper delivers a detailed summary of commonly used strategies in the direction of enhancing the free volume, nanophase-separated structure, and multi-stage proton transfer channels of PBI membranes. The main strategies in polymer molecular structure optimization are polymer main chain and side group modification, cross-linking, blocking and branching, *etc*. The strategies for compounding with other materials are compounding with organic porous polymers, inorganic component filling, and ionic liquid modification, *etc*. In addition, structural optimization and compounding synergistic modification strategies are more expected. The preparation of highly anhydrous proton-conducting membranes by the above strategies is of great theoretical research and industrial value. Moreover, this paper also proposes some future directions based on the above common strategies.

2. Factors influencing nonaqueous proton conduction

As shown in Fig. 1b [45], the hydrogen was oxidized into a proton and electron at the anode, and then the proton travels through the PEM to allow the reaction to occur with oxygen and electron, finally, the water was generated. Based on those working principles, PEM functioned as a solid electrolyte to determine the diffusion kinetics of the proton. Grotthus mechanism is the main proton transportation mechanism in PA-doped polymers [30,36,46]. Therefore, from the polymer membranes perspective, the factors influencing polymer structure and physicochemical properties exhibit a vital influence on the nonaqueous proton conduction, which can be categorized into the following three aspects: the number of phosphoric acids doping sites, the long-term retention rate after phosphoric acid doping, the balance and relationship between proton conductivity and mechanical properties [45–47].

The detailed factors influencing nonaqueous proton conduction can be found in Supporting information (S2.1–S2.3).

3. Strategies

3.1. Increasing free volume for more PA doping sites

The gap of the polymer molecular chain, which is defined as free volume (FV), plays a crucial role in phosphoric acid doping level [28,48,49]. There are several strategies for enriching the free volume of the PBI, for example, optimizing physicochemical properties and introducing the pendant groups, manipulating the branched structure, filling the inorganic component, and combining with the porous organic polymers.

3.1.1. Optimizing physicochemical properties and introducing the pendant groups

The optimizing physicochemical properties can be found in Supporting information (S3.1.1).

Graft modification of the molecular structure of PBI is also an effective method to improve proton conductivity [50], including hydroxylation [51], fluoridation [26], aromatic etherification [15], pyridine bridging oxygen connection [52], *etc*. For example, fluoridation could enhance chemical stability and increase solubility [26]. Introducing asymmetric bulky functional pendent groups, such as phenyl and methylphenyl could hold large free volumes, thus increasing the proton conductivity [53]. Furthermore, to offer the bonding sites with the crosslinker, it usually grafts the PBI with hydroxyl groups [51,54]. In this way, the proton conductivity could be maintained or improved indirectly. The processability and solubility of PBI could be enhanced by aromatic etherification [15]. In addition, As shown in Figs. 2a–c, the pyridine-bridged-oxypolybenzimidazole (PyOPBI) was concentrated to mitigate dissolution in 85% phosphoric acid. Tushar Jana has demonstrated that it was entirely steady in 85% PA [52]. Introducing the bipyridine group into the PBI membranes also showed improved nonaqueous proton conduction and fuel cell performance for that the bipyridine group could afford extra basic sites to loading more PA [55].

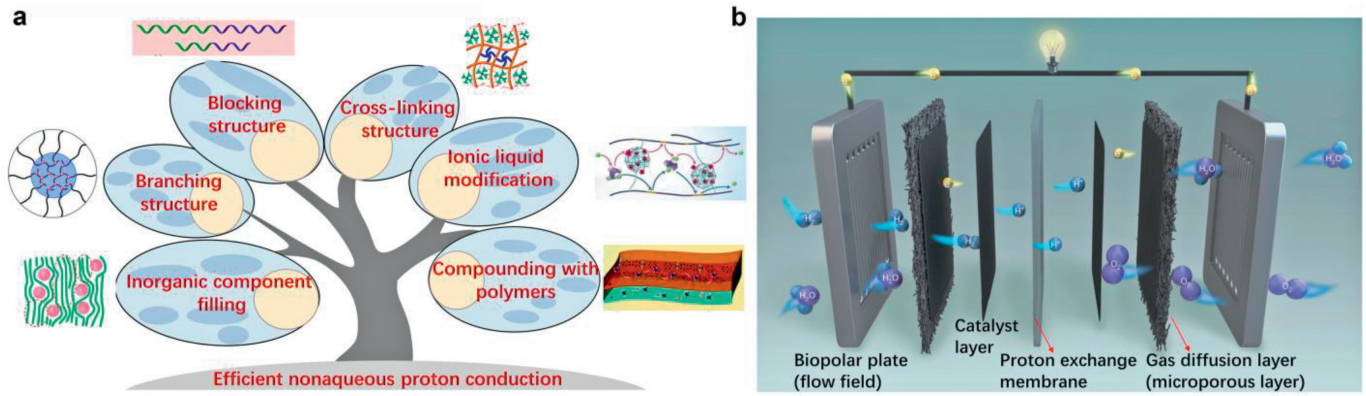

Fig. 1. (a) Schematic illustration of the main points of this review. Inorganic component filling. Reproduced with permission [39]. Copyright 2015, Wiley Publishing Group. Branching structure. Reproduced with permission [40]. Copyright 2020, Elsevier. Blocking structure. Reproduced with permission [41]. Copyright 2014, American Chemical Society. Cross-linking structure. Reproduced with permission [42]. Copyright 2020, American Chemical Society. Ionic liquid modification. Reproduced with permission [43]. Copyright 2018, Elsevier. Compounding with polymers. Reproduced with permission [44]. Copyright 2021, Royal Society of Chemistry. (b) A schematic explanation of the working principle. Reproduced with permission [45]. Copyright 2021, Springer Nature Limited.

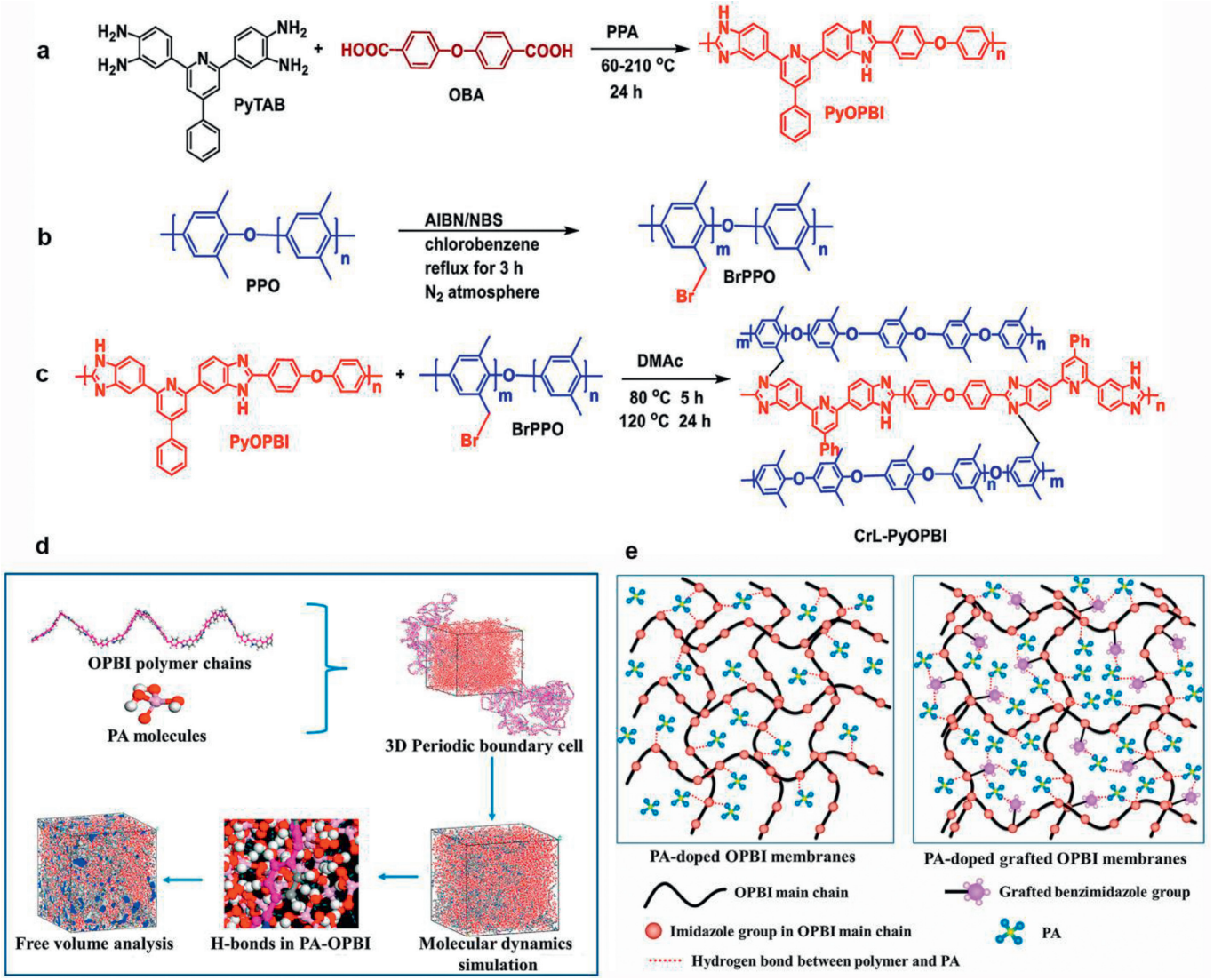

Fig. 2. Synthesis of (a) PyOPBI, (b) BrPPO, and (c) formation of the cross-linked polymer (CrL-PyOPBI) through the alkylation reaction between PyOPBI and BrPPO. Reproduced with permission [52]. Copyright 2020, American Chemical Society. (d) Models for molecular dynamics of PA doped oxypolybenzimidazole (OPBI). (e) The molecular chain stacking structure and hydrogen bond network of PA doped OPBI and grafted OPBI membranes. Reproduced with permission [58]. Copyright 2021, Elsevier.

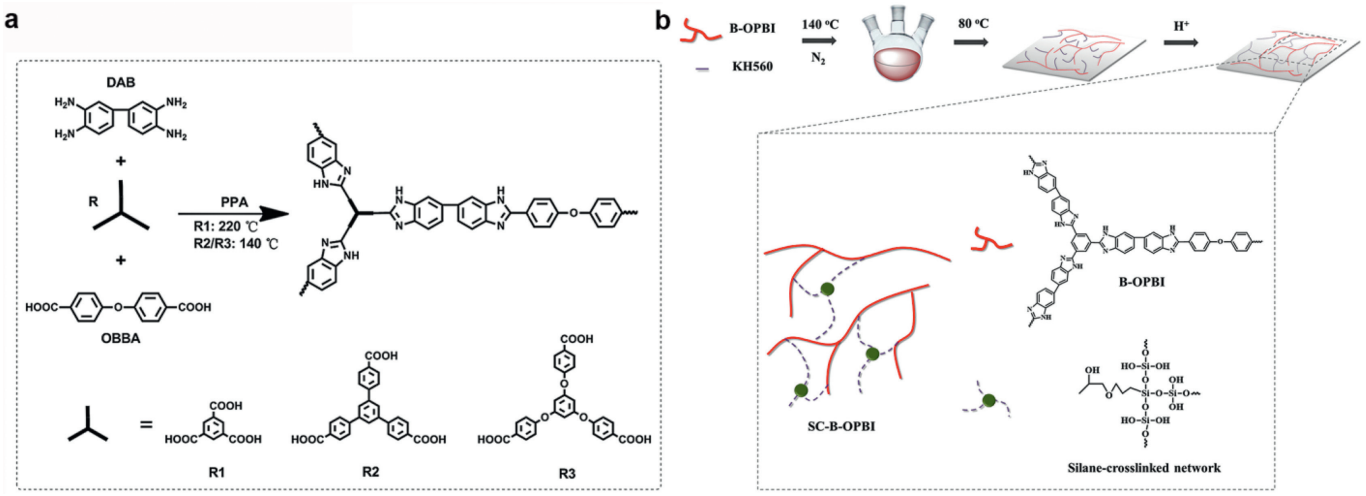

Fig. 3. (a) Synthetic routes and chemical structures of the different branched OPBIs. Reproduced with permission [71]. Copyright 2018, Elsevier. (b) Preparation of the SC-B-OPBI membrane. Reproduced with permission [72]. Copyright 2018, Elsevier.

Recent progress has suggested that introducing asymmetric bulky pendants is of paramount importance in increasing the FV [56,57]. Liu *et al.* proposed a novel method to graft the phenyl and methylphenyl to the molecular chain of the PBI [53]. Combined with the flexible ether linkages, the generated composite membrane holds large FV, and thus, enhanced proton transportation. The molecular simulation indicates that the larger FV originates from the looser molecular chain accumulation induced by the random and flexible framework of the PBI, and the larger steric-hinerance effect of phenyl and methylphenyl.

Furthermore, as shown in Fig. 2d, molecular dynamics (MD) simulation is an efficient theoretical tool for studying PA-doped membranes. As can be seen from Fig. 2e, MD simulation indicates that compared with the original OPBI membrane, the additional benzimidazole groups introduced into OPBI increases the free volume and promotes the uptake of PA, increasing the number of hydrogen bonds between PA and OPBI and thus enhancing the proton conductivity from 0.031 S/cm to 0.101 S/cm at 160 °C [58]. Moreover, there are many strategies to tailor the molecular structure of the noncommercial PBIs, such as incorporation nitrogen containing heterocycles [59–62], sulfonate [63–66], hydroxyl [60,67], and amino groups [68–70].

3.1.2. Establishing branched structure

Regarding the strategy used for the function of PBI's structure to increase the FV, the abundant tunable molecular structure could be harvested in the manner of establishing a branched structure. Using the function of attenuating the strong interactions between mainchains of PBI, increasing the solubility, and enhancing the FV, establishing a branched structure is beneficial for modulating the ADL and proton transportation. In this approach, Wang *et al.* have made many successful attempts, they investigated the influence of different branch structures and the degree of branch structure on the properties of PBI [71]. In general, as shown in Fig. 3a, three branching agents were used to clarify the relationship between the branching structure and the proton conductivity. Under the condition of the same degree of branching (DB), the OPBI-R2 affords the largest content of FV, and thus, the highest value of acid doping level (8.94), and the highest deformation ratio (1.5%), so the proton conductivity could be 0.053 S/cm under 180 °C without humidification. These excellent properties could be attributed to the effect of the rigid framework of the R2 which possesses a large volume. The detailed comparison of overall characteristics can be seen in Table S1 (Supporting information). Moreover, with the DB increasing, the density of the composite membranes decreased, and thus, the FV would be improved, so the proton transfer would be facilitated significantly due to the largely enhanced ADL. Regarding this aspect, establishing a branched structure is an ingenious approach to add the FV, and the characteristics of the branched PEMs could be manipulated controllably by altering the branching agents and the DB. Furthermore, the branched structure could also improve the antioxidation capability and durability.

On the other hand, the drawback of introducing the branched structure would damage the mechanical strength to some extent. To solve the problem, the strategy of the combination of crosslinking and mediating branched structure would afford significant advancements. From this approach, as shown in Fig. 3b, Wang's group synthesized the poly[2,2′-(*p*-oxydiphenylene)-5,5′-benzimidazole] (B-OPBI) membrane which possessed the branching structure with a branching degree of 6%, and then the γ-(2,3-epoxypropoxy)propyltrimethoxysilane (KH560) was used as the crosslinker. Such a composite membrane holds the merits of crosslinking and branching structure [72].

The crosslinking endows the membrane with an applicable tensile strength (78.4 MPa), while the branching structure contributes to a superior proton conductivity (0.044 S/cm, 180 °C, 0%RH). In addition, the synergistic effect of crosslinking and branching structure gives rise to a fair-sized mitigation of PA leaching. Because of the enhanced proton transfer, these modified PBI-based membranes exhibited vastly improved overall performance of the fuel cell.

The synergy of multiple modification strategies is crucial within composite membranes based on branched PBI. Wang *et al.* incorporated the proton conductor UiO-66 and the plasticizer ionic liquid (IL) ([BMIM][TFSI]) into branched CBOPBI. Despite the strong interfacial modification effect of IL, the tensile strength was retained at 40 MPa even when the content of UiO-66 was increased to 50%. This approach yielded a proton conductivity of 0.135 S/cm and a power density of 736 mW/cm^2 at 160 °C and 0%RH, along with establishing high-density proton transfer pathways [73].

3.1.3. Compounding with organic porous polymers

Another effective method to increase the free volume is to combine the crystalline porous materials with polymer. In addition to metal–organic frameworks (MOFs) and covalent organic frameworks (COFs), coordination polymers and polyoxometalates are also better candidates (Fig. S1a in Supporting information) [74–

79]. Each of these materials has the feasibility to be compounded with polymers and the structure can be designed precisely.

The detailed explanation of compounding with MOFs and COFs (Figs. S1b–e) can be found in Supporting information (S3.1.3-1).

In addition to traditional composite methods, such as physical blending and mechanical doping, the strategy of constructing integrated polymer have harvested extensive applications because they can eliminate the utilization of additional fillers or bonding agents that mainly cause unexpected material agglomeration and interface separation. The hybridization form of the membranes plays a critical function in deciding the efficiency of the proton conduction, as an integrated structure usually establishes multi-stage proton transfer channels [80].

Furthermore, Wang *et al.* adopted a soft-rigid synergistic strategy for *in situ* grafting of a rigid structure of COF-316 containing cyano groups onto a soft OPBI substrate. The resulting composite membrane contained multi-stage proton transfer channels while retaining a tensile strength of 12.1 MPa and delaying the dissolution of PA. Consequently, the membrane exhibited high proton conductivity (0.178 S/cm) and power density (774.7 mW/cm^2) at 160 °C without humidification [17].

In particular, when polymers are combined with crystalline porous polymers, more attention is paid and optimized to the stability of the composite film in the absence of water or at high temperatures and to the processability of the film formation.

The detailed explanation of incorporation with polymers of intrinsic microporosity (Fig. S2) can be found in Supporting information (S3.1.3–2).

In addition to compounding with organic porous polymers. Of particular note is manipulating polymer with intrinsic microporosity for building more free volume to enhance PA retention. As shown in Figs. 4a and b, by using Tröger's base-derived polymers synthesized with an average radius of 3.3 Å intrinsic ultramicropore, the siphoning effect of the intrinsic ultramicropore and the acid-base interaction between the polymers and phosphoric acid can greatly enhance the PA doping level and retention rate, guaranteeing the efficient proton conductivity at −20–200 °C and enabling the fuel cell to operate in this wide temperature range [48,81]. And the 3D observation of the DMBP-TB modeled structure in a non-crystalline cell is shown in Fig. 4c. Benefiting from the intrinsic ultramicropore, the unique membrane exhibited high proton conductivity of 0.159 S/cm at 180 °C and a peak power density of 815 mW/cm^2 at 160 °C.

The achievement of PEMFC electric cars has led to a strong interest in efficient proton conduction in proton exchange membranes over a wide temperature range (40–200 °C) [82,83]. An elaborately modularized abundant hydrogen-bonded three-dimensional crosslinked porous network polyacrylamide (PAM) hydrogels layers were imported into OPBI [44]. As a result, the rational modulation of double-layer composite film to mitigate the poor strength and high dimensional swelling of PAM and enhance absorption of PA and water represents efficient proton conduction between 40 °C and 180 °C. Proton transportation pathways in PA-doped composite membranes are shown in Fig. 4d, at low temperatures (<80 °C), water mainly serves as a medium for continuous proton conduction, while at high temperatures (>160 °C), the hydrogen bonding network between imidazole groups of OPBI, polyacrylamide, and phosphoric acid contributes to efficient nonaqueous proton conduction. As shown in Figs. 4e and f, the membrane of OPBI-0.8AM affords the proton conductivity of 0.0159 S/cm at 40 °C and 0.104 S/cm at 180 °C with water-free condition and exhibits a peak power density of 560 mW/cm^2 at 160 °C and 0%RH.

3.1.4. Inorganic component filling

The detailed explanation of inorganic components filling (Fig. S3) can be found in Supporting information (S3.1.4).

3.2. Establishing nanophase-separated structure for more PA doping sites

Establishing a nanophase-separated structure is a very fantastic method to facilitate proton transportation and largely augment the performance of fuel cells. In general, the three-dimensional penetrating proton transfer roadway provided by the nanophase-separated structure allows for more intense reaction kinetics. As shown in Fig. S4 (Supporting information), considering the design principle of "couple hardness with softness", constructing the block copolymer PBI membranes using two distinct polymers containing the inflexibility (diamine-terminated polybenzimidazole) and soft backbones (acid-terminated polybenzimidazole) [49]. In this way, nanophase-separated membranes were successfully synthesized. It represents a proton conductivity of 0.1 S/cm at 180 °C and a maximum power density of 360 mW/cm^2 at 160 °C without humidification due to regulated continuous proton nanochannels and optimized mechanical properties. Moreover, there are many block copolymers, for example, *para*-polybenzimidazole (*p*-PBI) combined with meta-polybenzimidazole [41], sulfonated PBI-*block*-*p*PBI [84], poly(arylene ether sulfone) coupled with polybenzimidazole [85].

3.3. Composite methods for improving the long-term retention rate after phosphoric acid doping

Equally important as a high ADL in improving the proton transfer efficiency of composite films is the long-term retention rate after phosphoric acid doping, so reducing the loss rate after phosphoric acid doping is also of high strategic importance, which is also a great challenge.

A well-established strategy is to introduce various nitrogen-containing functional groups into the PBI structure [42,58,86–89]. Considering the synthesis condition is also crucial for manipulating alkaline functional groups for the goal of environmental friendliness. A quaternized poly(4,4′-diphenylether-5,5′-bibenzimidazole) (OPBI) was synthesized using quaternary ammonium-functionalized epoxy with OPBI which avoids using the toxic agents and preserving the PBI structure (Fig. 5a). The quaternary ammonium moieties in OPBI's structure could largely enhance the ADL and attenuate the leakage of PA through strong acid-base interaction [90]. A proton conductivity of 0.085 S/cm at 160 °C can be obtained. Moreover, it possesses fantastic stability even running after 100 h. In addition, through an innovative approach, Wang *et al.* employed acid-etched UIO-66-NH_2 as a self-sacrificing reagent to construct additional carboxylated proton transport pathways. Combined with cross-linking and branched structures, these pathways substantially improved PA retention and enabled stable cycling for 387 h [91].

Another effective strategy is the composite method. Ionic liquids are a promising class of non-aqueous proton carriers in the field of proton exchange membrane, but they are difficult to solidify in membranes, so while improving non-aqueous proton conductivity, they also pose the problem of ionic liquids and doped phosphoric acid leakage [35,92,93]. Protic ionic liquids which are mainly based on ammonium and imidazolium are effective agents to improve nonaqueous proton conduction [5]. Similar to ionic liquids, the stability of PBI at high temperatures and the probability to design the molecular structure accurately have attracted many researchers. The combination of protonated ionic liquids and PBI offers unlimited possibilities for the construction of highly anhydrous proton-conducting membranes.

As shown in Fig. 5b, a composite membrane consisting of polybenzimidazole containing hydroxyl groups and 1–butyl–3-methylimidazolium dihydrogen phosphate was manipulated. It is evident that the incorporation of a cage-like cross-linked structure

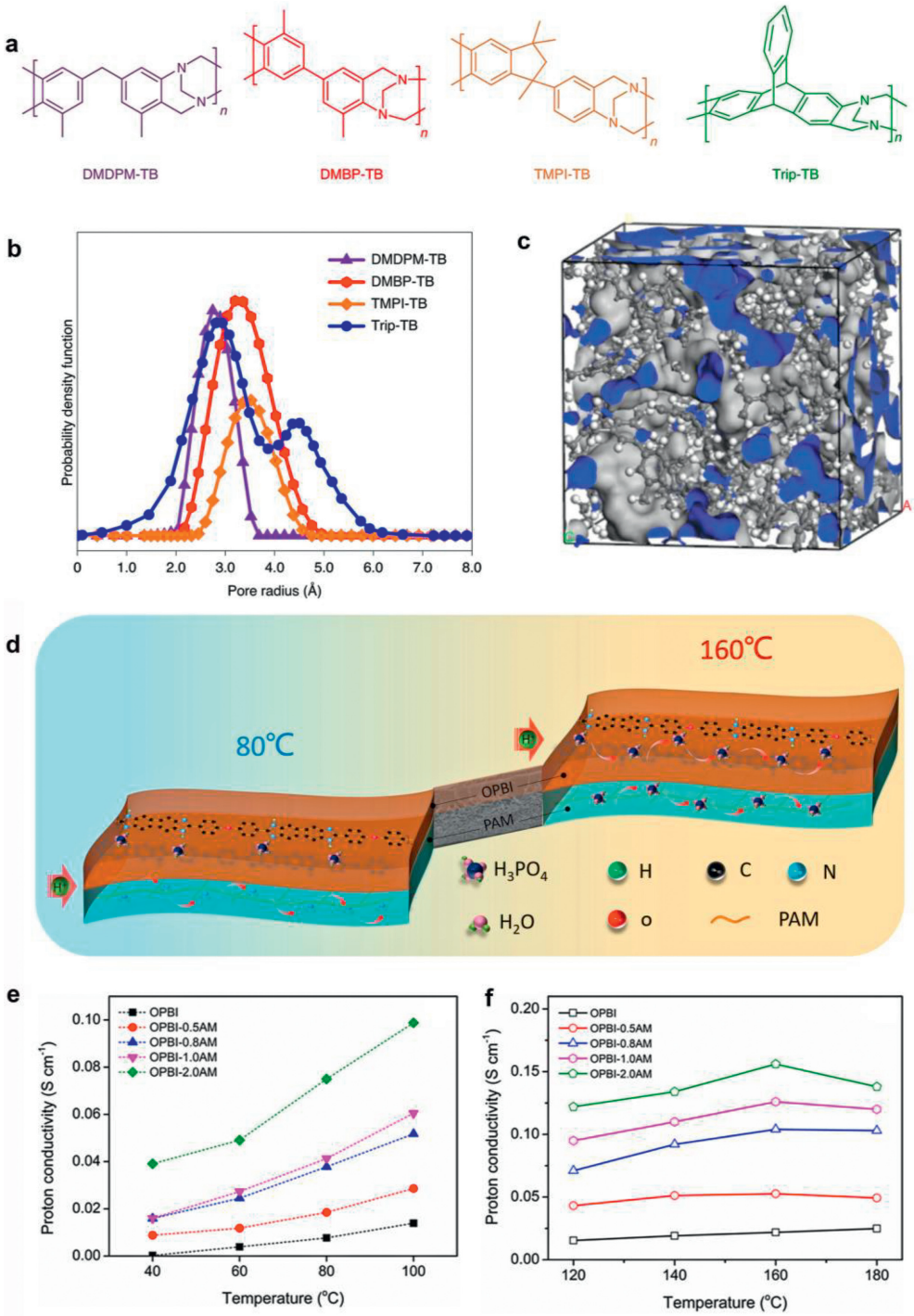

Fig. 4. Chemical structures and properties of TB polymers. (a) Structures of four different TB polymers. (b) Pore-size distributions obtained *via* CONTIN analysis from PALS. (c) 3D view of DMBP-TB modeled structure in an amorphous cell (308 K). (Cell size: 25.2 × 25.2 × 25.2 Å^3; density of ~1.031 g/cm^3. Gray, van de Waals surface; blue, Connolly surface with pore radius of 1.0 Å.) Reproduced with permission [48]. Copyright 2022, Springer Nature Limited. (d) Schematic representation of proton conduction pathways in PA-doped OPBI-AM membranes. The proton conductivity of the membranes at (e) low temperature and (f) high temperature. Reproduced with permission [44]. Copyright 2021, Royal Society of Chemistry.

which is enabled by the addition of 3-(triethoxysilyl)propyl isocyanate (IPTS) could largely relieve the leakage of ionic liquids and PA. Beside, it brings up some gratifying merits. The combination of a unique cage-like structure and imidazole rings enriched ionic liquid constructs multi-stage proton transfer channels, which greatly enhances proton conductivity (0.133 S/cm at 160 °C) and stability [43]. It is noteworthy that the protons in the protonated poly ionic liquid are present on the anion through a two-step ion exchange interaction.

The poly ionic liquids derivates from the free radical polymerization of ionic liquid afford cross-linked structure with the norbornene monomer of NbPBI and they exhibited various chain packing tightness due to the different functional groups (Fig. 5c). Different from traditional ionic liquids, Wang *et al.* proposed three novel double bond ionic liquids that simultaneously act as cross-linker and proton carriers as shown in Figs. 5d and e [94]. As a result, those composite membranes show improved PA retention rate (87.2% under 160 °C for 400 h) and enhanced proton conductivity

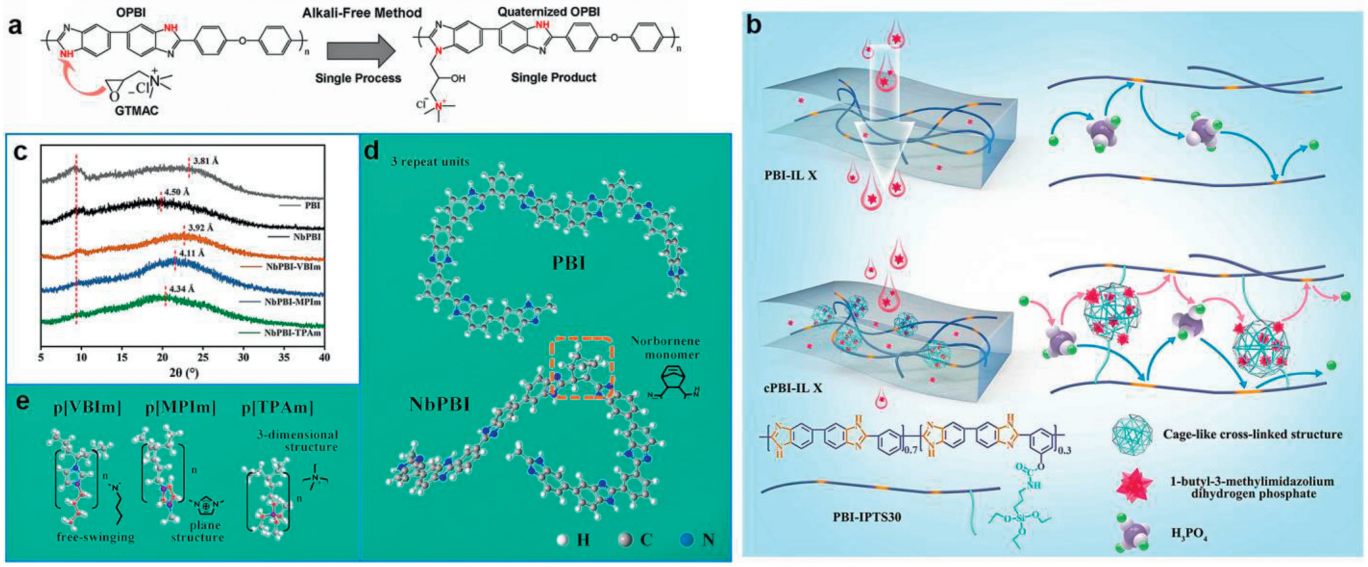

Fig. 5. (a) Synthetic process of quaternized PBI using the alkali-free approach. Reproduced with permission [90]. Copyright 2022, Elsevier. (b) Proton transporting path of cPBI-IL X membranes. Reproduced with permission [43]. Copyright 2018, Elsevier. (c) WAXD spectra of PBI, NbPBI and NbPBI-PIL membranes, (d) the polymer chains simulation of PBI and NbPBI, (e) the chemical structure of VBIm, MPIm and TPAm. Reproduced with permission [94]. Copyright 2018, Elsevier.

(0.074 S/cm at 170 °C). A power density of 385 mW/cm^2 at 160 °C can be achieved for fuel cells with NbPBI-TPAm membrane. Furthermore, the durability test at 300 mA/cm^2 shows that the composite membrane has excellent stability over 200 h of operation.

3.4. Cross-linking strategies for compromising between proton conductivity and mechanical strengths

The mechanical strengths of the PEM will suffer great damage when the ADL is very high owning to the plasticizing effect of PA. For another, the PA leaching would be severe. Thereafter, the balance between proton conductivity and mechanical strengths remains a challenge [38]. Electrostatic spinning and crosslinking are effective strategies for providing the composite membranes with robust mechanical properties and preventing PA leaching [95–97]. The porous structure formed by electrostatic spinning can increase the doping level of phosphoric acid and improve proton conductivity. However, the method has a limited improvement in mechanical properties and the membrane is less flexible, which is difficult to improve the overall performance of the membrane [98,99].

The crosslinking consists of ionically crosslinking and covalently crosslinking [100]. Covalent cross-linking usually endows composite films with high mechanical strength and excellent chemical stability [26]. Ionic cross-linking facilitates the construction of nano-phase separated structures which can enhance proton conduction [101]. In general, the ionically crosslinking is not beneficial for thermal stability, while covalently crosslinking exhibited low elongation at break when using the small-molecular crosslinkers [102].

3.4.1. Ionic cross-linking strategies

The detailed explanation of ionic cross-linking strategies (Fig. S5) can be found in Supporting information (S3.4.1).

3.4.2. Covalent cross-linking strategies

As a typical case, as shown in Fig. S6 (Supporting information), the crosslinking reaction between F_6-PBI and chloromethylated polysulfone was explored to acquire polymer crosslinked CrL-F_6-PBI membranes. The excellent merits of these crosslinking membranes permit higher ADL, and thus improved the proton conduction as well as robust tensile strength [26].

Therefore, regulation of the original crosslinker would boost the comprehensive properties of the composite crosslinking films. Moreover, as a novel cross-linking agent for PBI, pillar arene bearing multiple alkyl bromide molecules enables the establishment of a locally highly concentrated cross-linked PBI network. This optimization enhances the distribution state of the cross-linked units and synergistically enhances the FV and PA absorption capacity. This approach, combined with the stacking of the loosely packed PBI chain segments, achieved an impressive proton conductivity of 0.242 S/cm and an exceptionally high power density of 1084 mW/cm^2 at 180 °C [103].

4. Conclusions and prospects

4.1. Conclusions

The advantages of HT-PEMFCs in terms of higher catalyst efficiency, higher tolerance of fuel impurities, and simplified water/heat management make them more suitable for driving heavy-duty vehicles. The green and sustainable electrification of the automotive industry has also accelerated the commercialization of HT-PEMs. Continued research on high-temperature proton exchange membranes has led to significant advances in anhydrous proton conductivity, mechanical properties, and fuel cell performance.

This review summarizes several common strategies used to improve the anhydrous proton conductivity of PEMs (Table S2 in Supporting information) and suggests future directions for improvement. The key points of these strategies are to increase the free volume and nano-phase separated structure and enhance the acidic sites while maintaining good mechanical properties to enhance the proton conduction sites and maintain the long-period proton transportation. However, the current optimization steps for polymer molecular structure are tedious, and the construction of composite membranes is difficult to achieve hybridization at the molecular level. Therefore, the performance of polymer membranes in fuel cells is not perfect, thus, hindering their practical application.

Excessive PA uptake will sacrifice the mechanical properties of the membrane to some extent, so it needs to be quantitatively regulated to precisely optimize the composite membranes. A more flexible approach is to achieve high proton conductivity at low PA

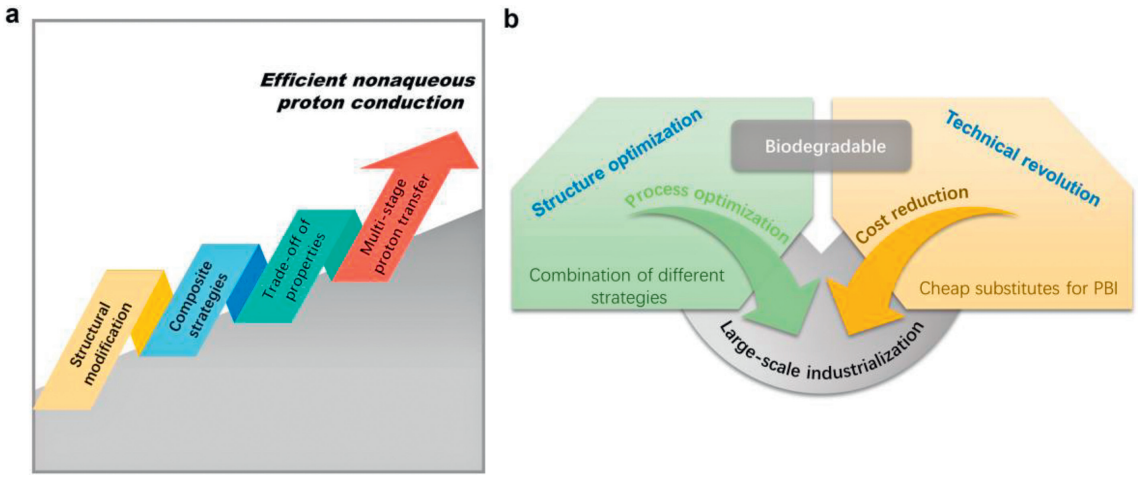

Fig. 6. (a) Steps to achieve efficient nonaqueous proton conduction and (b) prospects to achieve large-scale industrialization.

doping without loss of mechanical strength by introducing multi-stage proton transfer channels.

Furthermore, many modification strategies are laboratory level, and there will be many process issues to be settled when they are scaled up for industrial engineering, therefore, the modification strategies should be more suitable for industrial scale-up. Fig. 6a shows the comprehensive optimization steps to achieve efficient nonaqueous proton conduction.

4.2. Prospects

Carbon emission is a global problem, and how to reduce carbon emissions is a problem that is being addressed from the national level to the energy industry, automotive industry, transportation industry, and other related fields. In particular, the development of HT-PEMFCs in heavy-duty vehicles is of strategic importance in terms of cost reduction, efficiency, and emission reduction. Efficient anhydrous proton conduction will help accelerate the development of energy and heavy-duty transportation technologies.

In future research, optimization of the polymer structure itself will be the priority, and subsequent optimization can be continued in combination with other strategies on this modified polymer structure. Surface functionalization of the filled inorganic component potentially allows effective hybridization of the composite membrane with an inorganic component at the molecular level and avoids the problem of particle detachment in the membrane during long cycle runs. For organic-inorganic composite membranes, two strategies can be adopted in the future to increase the interfacial compatibility between filler and membrane substrate to enhance the anhydrous proton conductivity under the long-cycle operation of fuel cells. Surface modification of inorganic components with coupling agents to build a "core-shell" structure filler and with ionic liquids to enrich the surface with functional groups.

The construction of branching-block PBI copolymers may be a preferred approach to improve the proton conductivity and other comprehensive properties of PBI-based HT-PEMs because it can increase the FV of the membrane, maintain the PA doping sites, and build nano-phase separated structures. This modification strategy can enhance the proton conductivity while maintaining the good compromise between proton transfer efficiency and mechanical strengths. The establishment of branch-block PBI copolymers still has a large scope for research and enhancement.

Using advanced characterization techniques such as *quasi*-elastic neutron scattering and solid-state Nuclear Magnetic Resonance, combined with density functional theory to detect the mechanism of proton conduction, which in turn feeds into the structural design of the material to optimize the proton transport paths.

New cross-linking agents will effectively avoid the reaction and consumption of N-H sites (acid doping sites) and endow the composite membrane with less organic dissolution, outstanding antioxidant ability, enhanced mechanical properties, and higher acid doping levels.

Among the IL modification strategies, it is expected to solve the problem of ionic liquid leaching in membranes and to focus on the construction of multi-stage proton transfer channels.

Compounding with organic porous polymers can significantly enhance the proton conduction of the PEM, but more attempts should be made to modulate the polymer itself into a structure with abundant micropores, which can increase the free volume, and at the same time, taking advantage of the siphon effect of the micropores and acid-base interactions to improve the doping level and long-term retention rate of phosphoric acid, while taking care not to lose the mechanical properties of the membrane.

More than anything else, it requires a combination of the above strategies and ensures that the proton conductivity is enhanced without losing other excellent overall performance.

The organic combination of the above strategies has a tremendously positive effect on enhancing the behavior of HT-PEMFCs, which will also attract more attention to the research and industrialization of its related technologies to land, solve the bottlenecks of today's applications, and accelerate the large-scale applications in the near future.

Finally, the high cost of PBI and its analogs is the fatal drawback that hinders its large-scale industrialization, while the new structure of PBI analogs also has the bottleneck of high processing difficulty because of the solubility problem. Therefore, the future should be developed from two aspects, one is to reduce the production cost of PBI while looking for cheap substitutes for PBI, and more importantly, to develop cheap biodegradable HT-PEMs, for example, polyvinyl alcohol and polyvinylpyrrolidone (Fig. 6b).

Declaration of competing interest

The authors declare that they have no known competing financial interests or personal relationships that could have appeared to influence the work reported in this paper.

Acknowledgments

This work was supported by the Science Foundation of National Key Laboratory of Science and Technology on Advanced

Composites in Special Environments, and the National Natural Science Foundation of China (No. 12002109). This work was sponsored by Natural Science Foundation of Chongqing, China (Nos. CSTC2021jcyj-msxmX10305, CSTB2022NSCQ-MSX0246, CSTB2022NSCQ-MSX0242, CSTB2022NSCQ-MSX1244, CSTB2022NSCQ-MSX0441, CSTB2022NSCQ-MSX1356, CSTB2022NSCQ-MSX1572, CSTB2022NSCQ-MSX1583, CSTB2022NSCQ-MSX0487, CSTB2022TFII-OFX0034), and Chongqing Technology Innovation and Application Development Special Key Project (No. CSTB2023TIAD-KPX0010).

Supplementary materials

Supplementary material associated with this article can be found, in the online version, at doi:10.1016/j.cclet.2023.109261.

References

[1] Y. Jin, T. Wang, X. Che, et al., J. Power Sources 526 (2022) 231131.
[2] X. Liu, J. Zhang, C. Zheng, et al., Energy Environ. Sci. 13 (2020) 297–309.
[3] S.S. Araya, F. Zhou, V. Liso, et al., Int. J. Hydrog. Energy 41 (2016) 21310–21344.
[4] J. Yang, X. Li, C. Shi, et al., J. Membr. Sci. 620 (2021) 118855.
[5] H.A. Elwan, M. Mamlouk, K. Scott, J. Power Sources 484 (2021) 229197.
[6] D. Aili, J. Zhang, M.T. Dalsgaard Jakobsen, et al., J. Mater. Chem. A 4 (2016) 4019–4024.
[7] T. Søndergaard, L.N. Cleemann, H. Becker, et al., J. Power Sources 342 (2017) 570–578.
[8] E. Quartarone, S. Angioni, P. Mustarelli, Materials 10 (2017) 687–703.
[9] C. Laberty-Robert, K. Vallé, F. Pereira, C. Sanchez, Chem. Soc. Rev. 40 (2011) 961–1005.
[10] W. Wu, Y. Li, J. Liu, et al., Adv. Mater. 30 (2018) 1707516.
[11] S.H. Shin, A. Kodir, D. Shin, S.H. Park, B. Bae, Electrochim. Acta 298 (2019) 901–909.
[12] B. Liu, B. Hu, J. Du, et al., Angew. Chem. Int. Ed. 60 (2021) 6076–6085.
[13] J. Wang, P. Li, Y. Zhang, et al., J. Membr. Sci. 585 (2019) 157–165.
[14] M. Vinothkannan, R. Hariprasad, S. Ramakrishnan, A.R. Kim, D.J. Yoo, ACS Sustain. Chem. Eng. 7 (2019) 12847–12857.
[15] X. Li, H. Ma, H. Wang, et al., RSC Adv. 5 (2015) 53870–53873.
[16] T. Wang, Y. Jin, T. Mu, T. Wang, J. Yang, J. Membr. Sci. 654 (2022) 120539.
[17] J. Peng, X. Fu, D. Liu, et al., J. Membr. Sci. 655 (2022) 120603.
[18] J. Jung, J. Ku, Y.S. Park, et al., Polym. Rev. 62 (2022) 789–825.
[19] X. Hao, Z. Li, M. Xiao, et al., J. Mater. Chem. A 10 (2022) 10916–10925.
[20] F. Arslan, K. Chuluunbandi, A.T.S. Freiberg, et al., ACS Appl. Mater. Interfaces 13 (2021) 56584–56596.
[21] G. Wang, J. Li, H. Li, et al., Chin. Chem. Lett. 34 (2023) 107497.
[22] D. Aili, D. Henkensmeier, S. Martin, et al., Electrochem. Energy Rev. 3 (2020) 793–845.
[23] J.S. Artimani, M. Ardjmand, M. Enhessari, M. Javanbakht, J. Polym. Res. 27 (2020) 346–361.
[24] S. Mukhopadhyay, A. Das, T. Jana, S.K. Das, ACS Appl. Energy Mater. 3 (2020) 7964–7977.
[25] S. Angioni, P.P. Righetti, E. Quartarone, et al., Int. J. Hydrog. Energy 36 (2011) 7174–7182.
[26] J. Yang, Q. Li, L.N. Cleemann, et al., Adv. Energy Mater. 3 (2013) 622–630.
[27] Y.L. Ma, J.S. Wainright, M.H. Litt, R.F. Savinell, J. Electrochem. Soc. 151 (2004) A8–A16.
[28] P. Wang, Z. Liu, X. Li, et al., Chem. Commun. 55 (2019) 6491–6494.
[29] R. Haider, Y. Wen, Z.F. Ma, et al., Chem. Soc. Rev. 50 (2021) 1138–1187.
[30] J.A. Asensio, E.M. Sánchez, P. Gómez-Romero, Chem. Soc. Rev. 39 (2010) 3210–3239.
[31] J. Zhang, D. Aili, S. Lu, Q. Li, S.P. Jiang, Research 2020 (2020) 9089405.
[32] J. Escorihuela, J. Olvera-Mancilla, L. Alexandrova, L.F. Del Castillo, V. Compañ, Polymers 12 (2020) 1861–1901.
[33] N. Esmaeili, E.M. Gray, C.J. Webb, ChemPhysChem 20 (2019) 2016–2053.
[34] K.S. Khoo, W.Y. Chia, K. Wang, et al., Sci. Total. Environ. 793 (2021) 148705.
[35] A. Alashkar, A. Al-Othman, M. Tawalbeh, M. Qasim, Membranes 12 (2022) 178–207.
[36] G. Li, W. Kujawski, E. Rynkowska, Rev. Chem. Eng. 38 (2022) 327–346.
[37] H. Chen, S. Wang, J. Li, et al., J. Taiwan Inst. Chem. E 95 (2019) 185–194.
[38] J. Yang, H. Jiang, J. Wang, et al., J. Power Sources 480 (2020) 228859.
[39] G. Nawn, G. Pace, S. Lavina, et al., ChemSusChem 8 (2015) 1381–1393.
[40] L. Wang, Y. Wu, M. Fang, et al., J. Membr. Sci. 602 (2020) 117981.
[41] S. Maity, T. Jana, ACS Appl. Mater. Interfaces 6 (2014) 6851–6864.
[42] Y. Wang, P. Sun, Z. Li, et al., ACS Sustain. Chem. Eng. 9 (2021) 2861–2871.
[43] X. Wang, S. Wang, C. Liu, et al., Electrochim. Acta 283 (2018) 691–698.
[44] B. Yin, Y. Wu, C. Liu, et al., J. Mater. Chem. A 9 (2021) 3605–3615.
[45] K. Jiao, J. Xuan, Q. Du, et al., Nature 595 (2021) 361–369.
[46] E. Qu, X. Hao, M. Xiao, et al., J. Power Sources 533 (2022) 231386.
[47] S. Ahmad, T. Nawaz, A. Ali, et al., Int. J. Hydrog. Energy 47 (2022) 19086–19131.
[48] H. Tang, K. Geng, L. Wu, et al., Nat. Energy 7 (2022) 153–162.
[49] L. Wang, Z. Liu, J. Ni, et al., J. Membr. Sci. 572 (2019) 350–357.
[50] I. Nicotera, V. Kosma, C. Simari, et al., J. Phys. Chem. C 119 (2015) 9745–9753.
[51] F. Liu, S. Wang, J. Li, et al., J. Membr. Sci. 541 (2017) 492–499.
[52] R.Nayak Harilal, P.C. Ghosh, T. Jana, ACS Appl. Polym. Mater. 2 (2020) 3161–3170.
[53] X. Li, H. Ma, Y. Shen, et al., J. Power Sources 336 (2016) 391–400.
[54] C.H. Shen, S.L.C. Hsu, J. Membr. Sci. 443 (2013) 138–143.
[55] M.R. Berber, N. Nakashima, J. Membr. Sci. 591 (2019) 117354.
[56] Y. Cui, S. Wang, D. Wang, et al., J. Membr. Sci. 637 (2021) 119610.
[57] J.C. Chen, P.Y. Chen, Y.C. Liu, K.H. Chen, J. Membr. Sci. 513 (2016) 270–279.
[58] Y. Xiao, S. Wang, G. Tian, et al., J. Membr. Sci. 620 (2021) 118858.
[59] J. Fang, X. Lin, D. Cai, N. He, J. Zhao, J. Membr. Sci. 502 (2016) 29–36.
[60] J. Yang, Y. Xu, L. Zhou, et al., J. Membr. Sci. 446 (2013) 318–325.
[61] S. Maity, T. Jana, Macromolecules 46 (2013) 6814–6823.
[62] X. Li, C. Liu, S. Zhang, G. Yu, X. Jian, J. Membr. Sci. 423-424 (2012) 128–135.
[63] J.A. Mader, B.C. Benicewicz, Macromolecules 43 (2010) 6706–6715.
[64] L. Sheng, H. Xu, X. Guo, et al., J. Power Sources 196 (2011) 3039–3047.
[65] D.C. Villa, S. Angioni, S.D. Barco, P. Mustarelli, E. Quartarone, Adv. Energy Mater. 4 (2014) 1301949.
[66] S. Angioni, D.C. Villa, S.D. Barco, et al., J. Mater. Chem. A 2 (2014) 663–671.
[67] S. Yu, B.C. Benicewicz, Macromolecules 42 (2009) 8640–8648.
[68] X. Li, C. Liu, S. Zhang, L. Zong, X. Jian, J. Membr. Sci. 442 (2013) 160–167.
[69] S. Bhadra, N.H. Kim, J.H. Lee, J. Membr. Sci. 349 (2010) 304–311.
[70] N. Xu, X. Guo, J. Fang, H. Xu, J. Yin, J. Polym. Sci. Part A: Pol. Chem. 47 (2009) 6992–7002.
[71] L. Wang, J. Ni, D. Liu, C. Gong, L. Wang, Int. J. Hydrog. Energy 43 (2018) 16694–16703.
[72] M. Hu, J. Ni, B. Zhang, S. Neelakandan, L. Wang, J. Power Sources 389 (2018) 222–229.
[73] P. Wang, J. Lin, Y. Wu, L. Wang, J. Power Sources 560 (2023) 232665.
[74] X. Meng, H.N. Wang, S.Y. Song, H.J. Zhang, Chem. Soc. Rev. 46 (2017) 464–480.
[75] M. Zeng, W. Liu, H. Guo, et al., ACS Appl. Energy Mater. 5 (2022) 9058–9069.
[76] Y. Liu, J. Chen, X. Fu, et al., J. Power Sources 507 (2021) 230316.
[77] M.J. Baran, M.E. Carrington, S. Sahu, et al., Nature 592 (2021) 225–231.
[78] X.M. Li, J. Jia, D. Yang, J. Jin, J. Gao, Chin. Chem. Lett. 35 (2024) 108474.
[79] J. Li, J. Wang, F. Shui, et al., Chin. Chem. Lett. 34 (2023) 107917.
[80] A. Kumar, J. Mater. Chem. A 8 (2020) 22632–22636.
[81] J. Liu, B. Yuan, N. He, et al., Energy Environ. Sci. 16 (2023) 1024–1034.
[82] B. Yin, R. Liang, X. Liang, et al., Small 17 (2021) 2103214.
[83] Q. Liu, X. Wang, X. Zhang, et al., J. Clean. Prod. 359 (2022) 131977.
[84] J.A. Mader, B.C. Benicewicz, Fuel Cells 11 (2011) 222–237.
[85] H.S. Lee, A. Roy, O. Lane, J.E. Mcgrath, Polymer 49 (2008) 5387–5396.
[86] M. Hu, T. Li, S. Neelakandan, L. Wang, Y. Chen, J. Membr. Sci. 593 (2020) 117435.
[87] H. Bai, J. Zhang, H. Wang, Y. Xiang, S. Lu, J. Membr. Sci. 645 (2022) 120194.
[88] H. Guo, Z. Li, Y. Lv, et al., ACS Appl. Energy Mater. 4 (2021) 8969–8980.
[89] G. Venugopalan, K. Chang, J. Nijoka, et al., ACS Appl. Energy Mater. 3 (2019) 573–585.
[90] D. He, G. Liu, A. Wang, et al., J. Membr. Sci. 650 (2022) 120442.
[91] P. Wang, Y. Wu, W. Lin, L. Wang, J. Mater. Chem. A 10 (2022) 23058–23067.
[92] H.A. Elwan, R. Thimmappa, M. Mamlouk, K. Scott, J. Power Sources 510 (2021) 230371.
[93] F. Liu, S. Wang, H. Chen, et al., Renew. Energy 163 (2021) 1692–1700.
[94] F. Liu, S. Wang, D. Wang, et al., J. Power Sources 494 (2021) 229732.
[95] N. Nambi Krishnan, A. Konovalova, D. Aili, et al., J. Membr. Sci. 588 (2019) 117218.
[96] C. Charalampopoulos, K.J. Kallitsis, C. Anastasopoulos, et al., Int. J. Hydrog. Energy 45 (2020) 35053–35063.
[97] S. Jahangiri, İ. Aravi, L. Işıkel Şanlı, Y.Z. Menceloğlu, E. Özden-Yenigün, Polym. Adv. Technol. 29 (2018) 594–602.
[98] P. Muthuraja, S. Prakash, V.M. Shanmugam, P. Manisankar, Solid State Ionics 317 (2018) 201–209.
[99] H.Y. Li, Y.L. Liu, J. Mater. Chem. A 1 (2013) 1171–1178.
[100] J. Wu, S. Nie, H. Liu, et al., J. Mater. Chem. A 10 (2022) 19914–19924.
[101] W. Chen, T. Dong, Y. Xiang, et al., Adv. Mater. 34 (2022) 2108410.
[102] L. Wang, Z. Liu, Y. Liu, L. Wang, J. Membr. Sci. 583 (2019) 110–117.
[103] J. Peng, S. Wang, X. Fu, et al., Adv. Funct. Mater. 33 (2023) 2212464.